

Study on removal of microplastics using magnetic separation

Reo Ueda, Yoko Akiyama*, Yuichiro Manabe, and Fuminobu Sato

Graduate School of Engineering, Osaka University, Osaka, Japan

(Received 29 July 2022; revised or reviewed 29 August 2022; accepted 30 August 2022)

Abstract

In recent years, the impact of microplastics (MPs) on ecosystems is a serious problem. Since MPs are difficult to recover once they are dispersed into the environment, it is important to remove them at the source. We proposed a magnetic separation of primary MPs (plastics manufactured in minute sizes) sized 10-100 μm that has not been removed in the sewage process, based on the magnetic seeding process. In this study, we used magnetite as a magnetic seeding agent, and conducted magnetic separation experiments in the continuous process using a superconducting solenoidal magnet to investigate the feasibility of practical magnetic separation system of MPs. As a result, 85% separation rate was obtained by continuous separation using high gradient magnetic separation (HGMS) with hydrophobically treated magnetite as a magnetic seeding agent.

Keywords: microplastics, magnetic separation, superconducting solenoidal magnet, sewage treatment, continuous processing, magnetic seeding, surface treatment

1. INTRODUCTION

1.1. Technical Issues of Marine Microplastics.

Among the marine plastic debris, microplastics (hereinafter referred to as MPs) are large issue for their negative impact on ecosystems. MPs can be easily taken up into aquatic organisms [1, 2], causing feeding problems in their digestive systems and bioaccumulation of toxic chemicals [3, 4]. Generally, MPs are the plastic particles of 5 mm or less in size, and are classified into primary and secondary MPs. Primary MPs are plastics originally manufactured in microscopic size, and are mainly consists of spherical plastic grains (resin pellets) of several mm in diameter used as raw materials for manufacturing plastic products, and scrubbing agents (5 μm -1 mm) used in face washes, body soaps, toothpastes, etc. Primary MPs are discharged into the natural environment through domestic wastewater due to their fineness. Secondary MPs, on the other hand, are micro-sized plastic waste that has been degraded by external factors, resulting in crushing and fragmentation of the waste [5].

Plastics are discharged into the environment through various pathways. The three main pathways are: i) plastic waste leaks from landfills or is illegally dumped, ii) plastics existing on the roads and the soils are discharged into the ocean through rainwater and river, and iii) plastics in the domestic wastewater are discharged because they cannot be completely removed at sewage treatment plants. Unlike large plastics which can be recovered physically, efficient recovery methods have not been established for MPs that have already leaked into the environment. Therefore, to prevent further discharge of MPs into the environment, we focused on the pathway iii).

Tanaka et al. (2019) analyzed MPs larger than 100 μm by influent, effluent for four sewage treatment plants

(diversion type) in the Biwa Lake basin, and also investigated MPs larger than 10 μm for influent and effluent [6]. The concentration of MPs sized from 100 μm to 1 mm in the influent was 89 pieces/ m^3 and the treatment rate by the sewage treatment was 99.6%, while the concentration of MPs sized from 10 to 100 μm in the influent was 125,000 pieces/ m^3 and the treatment rate was 76.3%. Assuming a daily sewage inflow of 100,000 m^3 per a sewage treatment plant, this means that 3 billion MPs are discharged per day, or more than 1 trillion MPs per year. It is also known that PE is the major component of MPs sized 10 to 100 μm in the effluent, accounting for 46% of the total [7].

Based on this, we targeted the removal of MPs sized from 10 to 100 μm , which are primary MPs contained in domestic wastewater and passed through sewage treatment plants without being treated. The treatment flow, in which a magnetic separation process is added to sewage treatment, is shown in Fig. 1. To remove fine MPs remaining even after the final sedimentation tank, a magnetic separation process is installed as a final process. Whether the magnetic separation process will be used in place of or in combination with the rapid sand filtration should be considered depending on the actual sewage conditions.

1.2. Results of Small Batch Experiments and The Need For Continuous Processing.

In our previous study, we investigated the magnetic seeding method as one of the methods of magnetic separation [8]. A ferromagnetic material is attached to MPs contained in the sewage, and then a magnetic field is applied to the complex of MPs and ferromagnetic material to separate from the wastewater. The magnetic separation experiments for two types of MPs, polyethylene (PE) and polyamide (PA), were conducted in beaker-scale batch processing.

Magnetite particles (primary particle diameter 0.5 μm)

* Corresponding author: yoko-ak@see.eng.osaka-u.ac.jp

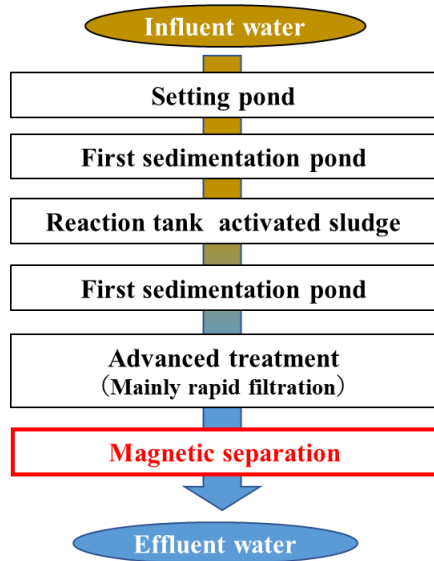


Fig. 1. An introduction example of magnetic separation to the sewage treatment process.

were added to simulated wastewater containing MPs, stirred, and then a magnetic field was applied from the bottom of the beaker by a small neodymium magnet (maximum flux density 0.4 T). As a result, separation rates were as high as 93% and 99% for PE and PA, respectively. The pH dependence of the zeta potentials respectively for PE, PA, and magnetite as the magnetic seeding agent, indicated that magnetite was positively charged whereas PE and PA were negatively charged around the neutral pH (pH=6), where the separation was performed. As the micrographs shown in Fig. 2, the magnetite particles found to be attached to the surface of both PE and PA. This indicates that magnetite particles naturally adhered to the MPs due to electrostatic interaction around neutral pH, making the magnetic separation in batch processing possible.

However, since our ultimate goal is to develop a magnetic separation system capable of separating MPs in the sewage, it is necessary to conduct the magnetic separation experiments for continuous treatment. Since the adhesion force between particles is an electrostatic interaction, which are weaker interactions than ionic and covalent bonds, there is a possibility that if a large magnetic or drag force acts on the MPs-magnetite aggregates during continuous treatment relative to the adhesion force between MPs and magnetite, these adhesions may detach and cannot be recovered due to magnetic forces.

Here, we conducted continuous processing experiments using two different methods: open gradient magnetic separation (OGMS) which uses the magnetic field gradient of the magnet itself, and high gradient magnetic separation (HGMS) in which a high gradient is formed by the arrangement of magnetic filters, to verify the possibility of continuous magnetic separation. Furthermore, to increase the adhesion between MPs and magnetite, continuous treatment experiments were conducted using hydrophobically treated magnetite as a magnetic seeding agent.

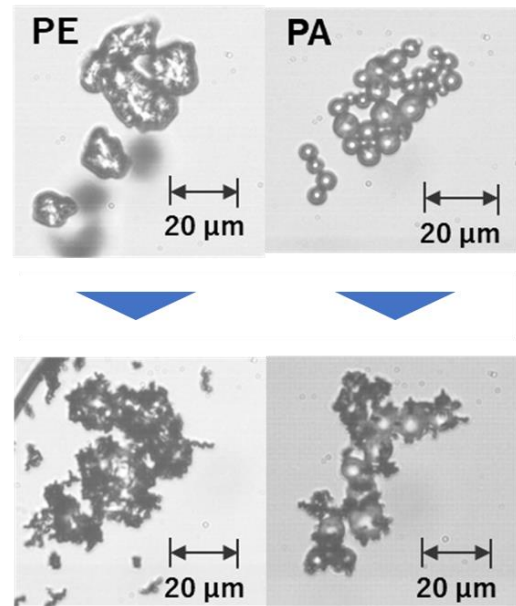


Fig. 2. Transmission micrographs of PE and PA particles before and after addition of magnetite.

2. MATERIALS AND METHODS

2.1. Separation of MPs by HGMS and OGMS

The effectiveness of continuous separation and recovery of MPs from simulated wastewater was investigated by attaching magnetite particles to MPs and passing them through a flow path in which a magnetic field is applied by a superconducting solenoidal magnet. A schematic diagram of the experimental system is shown in Fig. 3. In HGMS, the magnetic filters were installed in the magnet bore to increase the magnetic force acting on the particles, while in OGMS, a non-magnetic acrylic cylinder was placed in the bore.

The specifications of the superconducting solenoidal magnet used in the experiments are shown in Table I, and the experimental conditions are shown in Table II. Magnetic separation experiments were conducted for the simulated wastewater containing model MPs after addition of magnetite particles as the magnetic seeding agent and then stirring. The separation conditions in Table II was

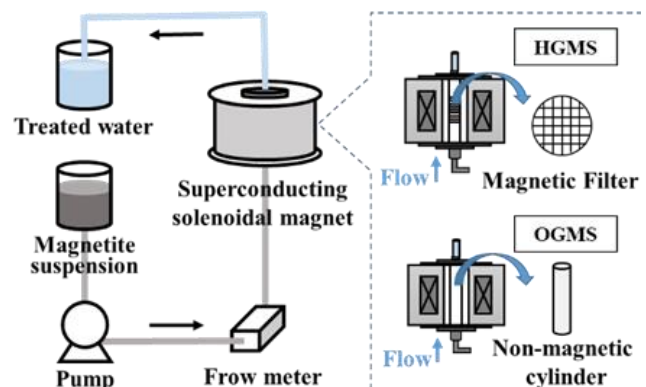


Fig. 3. Schematic diagram of continuous magnetic separation experiments using OGMS and HGMS.

TABLE I
SPECIFICATIONS OF SUPERCONDUCTING SOLENOIDAL MAGNET USED IN
MAGNETIC SEPARATION.

Magnet system	No refrigerant superconducting magnet
Model number	JMTD-10T100E3
Bore inner diameter	100 mm
Cryostat height	460 mm
Maximum center magnetic flux density	10 T
Cooling method	GM refrigerating
Superconducting wire rod	NbTi

TABLE II
MAGNETIC SEPARATION CONDITIONS BY HGMS AND OGMS FOR
CONTINUOUS PROCESSING.

Common	Flow rate	0.1 m/s
	Water amount	10 L
	Flow diameter	50 mm
	MPs concentration	0.5 g/L
	Magnetite concentration	0.5 g/L
HGMS	Filter material	Magnestain®
	Filter form	Plain weave
	Wire diameter	1 mm
	Mesh number	6
	Filter number	15
OGMS	Flow velocity	0.05, 0.10 m/s
	Magnetic field	0.5, 1.0, 3.0 T
	Flow velocity	0.05 m/s
	Magnetic field	6.0 T

determined by preliminary experiments and estimation of magnetic and drag forces acting on the particles.

As MPs, PA (polyamide, spherical polymer particles, KP-010, Kato Koken Co., Ltd., Japan 10 μm in particle diameter) were used to prepare simulated wastewater, and magnetite (Fe_3O_4) particles (primary particle size 0.5 μm , Sample B, Mitsui Mining & Smelting Co., Ltd., Japan) were used for magnetic seeding. Particle size distribution of PA and magnetite is shown in Fig. 4.

Under each condition, magnetic separation was performed for magnetite only and for a mixture of MPs and magnetite, respectively. After magnetic separation for each case, magnetite or the total weight of MPs adsorbing magnetite in the suspension passed through were weighed after vacuum filtration and drying at 60°C. On the other hand, all particles trapped on the walls of the filter or non-magnetic cylinder were collected and magnetite or the total weight of MPs adsorbing magnetite were weighed in the same manner. MPs separated was determined by subtracting the weight of magnetite from the total weight of MPs adsorbed with magnetite.

The separation ratio of magnetite and MPs were calculated by Equations (1) and (2), respectively.

$$\text{Separation rate of magnetite (\%)} = \frac{\text{Separation amount of magnetite (g)}}{\text{Input amount of magnetite (g)}} \times 100 \quad (1)$$

$$\text{Separation rate of MPs (\%)} = \frac{\text{Total separation amount (g)} - \text{Separation amount of magnetite (g)}}{\text{Input amount of MPs (g)}} \times 100 \quad (2)$$

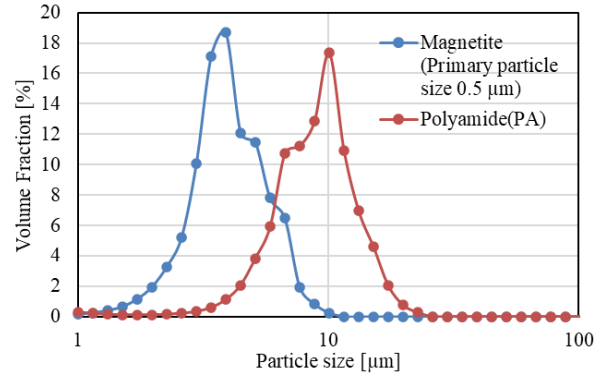


Fig. 4. Particle size distribution of magnetite and PA.

2.2. Separation of MPs Using Surface-Modified Magnetite.

As mentioned above, with untreated magnetite, the interaction between MPs and magnetite is basically an electrostatic interaction, which is weaker interaction than covalent or hydrogen bonds. So in the continuous processing, in case the magnetic force acting on the magnetite particle and the drag force acting on MPs are in different directions, the combined force of these forces may be larger than the adhesion force between MPs and magnetite, and magnetite is desorbed from MPs. It makes separation rate of MPs may decrease, even though pure magnetite can be recovered by magnetic separation. Thus, surface modification of magnetite particles with fatty acids was performed to enhance the adhesion between MPs and magnetite. Since the surface of MPs is generally hydrophobic, hydrophobization of the magnetite surface can increase these adhesion forces.

The binding of fatty acid ions to magnetite particles is shown in Fig. 5. Hydroxyl groups existing on the surface of magnetite particles can be modified by covalent bond through dehydration condensation with fatty acids. This covalent bond is maintained even after stirring in water. The length and shape of the modification groups can be controlled by changing the molecular weight and shape of the fatty acid.

In this study, based on preliminary experiments, caprylic acid-modified magnetite particles were used from two viewpoints: dispersibility of surface treated magnetite in water and adhesiveness to MPs. The procedure for the preparation of fatty acid-modified magnetite particles is as follows: 2.2×10^{-4} mol of sodium caprylate (sodium n-octanoate, special grade, Kishida Chemical Co., Ltd. Japan) was dissolved into 100 ml of distilled water heated to 90 °C using a thermostatic bath. The fatty acid solution was mixed using a stirring blade until completely dissolved, and then 0.10 g of magnetite particles with a primary particle size of 0.5 μm were added and allowed to react for 1 hour while continuing to stir and control the temperature.

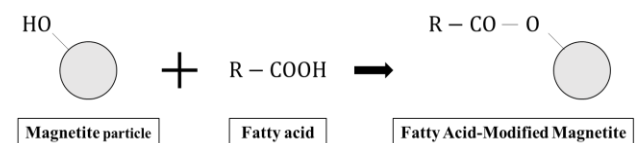


Fig. 5. Surface modification of magnetite particles by fatty acid ions.

After cooling the prepared particle dispersion at room temperature, magnetite particles were collected using a permanent magnet. The recovered particles were washed several times with distilled water and ethanol, and then dried at 70 °C using a constant-temperature dryer.

To investigate the degree of hydrophobization of magnetite particles by surface treatment, the contact angle against water was measured using a contact angle meter (Simple Mini7, Excimer Co., Ltd. Japan). The magnetite particles before and after treatment were formed into a diameter of $\phi 10 \text{ mm} \times 1 \text{ mm}$ by using a pelletizer. 8.2 μL of distilled water was dropped on the pellet and observed by CCD camera from the side to measure the height and width of the water droplets on the pellet, and the contact angle was calculated by a half-angle ($\theta/2$) method.

The obtained surface-modified magnetite was used for magnetic separation by HGMS under the same conditions as in section 2.1.

3. RESULTS AND DISCUSSIONS

3.1. Separation Rate of MPs by HGMS.

The PA separation rates obtained by HGMS under each condition are shown in Fig. 6. Here, "Pass" is the weight ratio of MPs passed through the magnetic separator against MPs input, whereas "Loss" is the weight ratio of MPs input minus passed and captured MPs against MPs input.

In all the experiments, the separation rate was lower than the PA separation rate of 93% to 99% in the magnetic separation experiments of the batch process. This is thought to be due to the shear force exerted on the particles by the magnetic or drag force, which is greater than the adhesion force between the MPs and magnetite particles, causing desorption of the magnetite particles from MPs.

Firstly, the results by HGMS is discussed. At 3T, the PA separation rates were about 35%, and no significant change was observed even by changing the separation rate. On the other hand, in experiments changing the magnetic field, separation rate increased up to 55% at 0.5 T. The shear forces acting on between the MPs and the magnetite

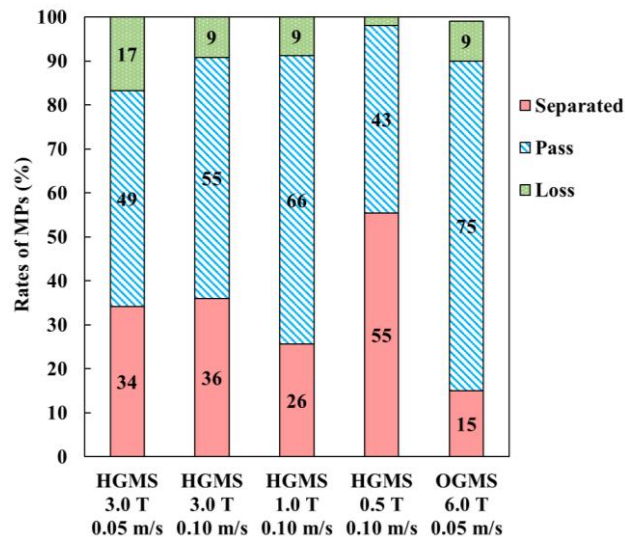


Fig. 6. Separation rate of MPs by HGMS and OGMS.

particles are magnetic and drag forces. So the fact that the separation rate increased with decreasing magnetic field even at a constant flow velocity suggests that desorption may be caused by magnetic forces greater than the adhesion force between MPs and magnetite particles when the magnetic field is large. In addition, partial blockage of the magnetic filter by magnetite particles was observed at 1T and 3T, suggesting that this blockage may have affected the separation rate. It has been confirmed in our previous other large-scale magnetic separation experiments that the blockage occurs at high magnetic fields when ferromagnetic materials are the target of HGMS separation [9, 10]. The blockage of magnetic filter causes local increase in the flow velocity, which may cause the particles to be swept downstream due to drag forces or large shear force is applied to the particles against the adhesion force between the MPs and magnetite.

The amount of separation per filter is shown in Fig. 7. In this figure, the first to fifth filters from the inlet side are labeled "1~5," the sixth to tenth are labeled "6~10," the eleventh to fifteenth are labeled "11~15," and the particles adhering to the cylinder wall are labeled "Walls". The effect of flow velocity at 3 T is negligible which is consistent with Fig.6. At 3 T and 1 T magnetic fields, most of the particles are captured by the 1-5th filters on the inlet side. On the other hand, when the magnetic field is decreased to 0.5 T, the amount of separation increases for filters 6~10 and 11~15, and "Wall" decreased, and the overall separation volume increased.

This suggests that the separation rate increased when the magnetic field was relatively small so that the particles could be captured uniformly on 15 filters, rather than being captured intensively on the filters on the inlet side, since no blockage occurred on the inlet side and the magnetic force acting on the particles did not exceed the adhesion force. The reason for the increase in the amount of adhesion on the cylinder wall at 3T and 1T compared to 0.5T is that the magnetic separation on the wall occurred on the inlet side due to the magnetic field gradient of the superconducting solenoidal magnet itself at large magnetic field.

3.2. Separation Rate of MPs by OGMS.

Next, the case with OGMS is discussed: preliminary experiments were conducted with OGMS to collect pure magnetite by varying the flow velocity and magnetic field,

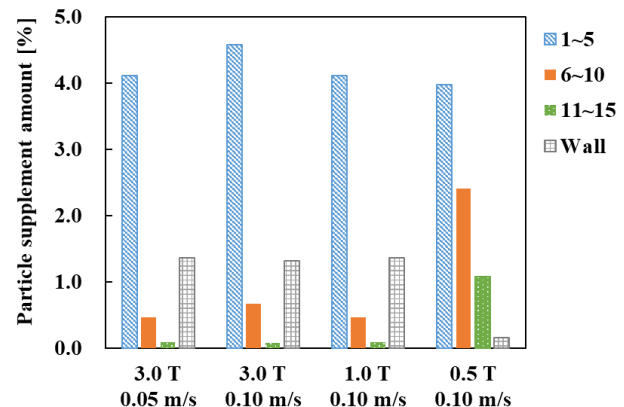


Fig. 7. Quantity of particles captured by each filter.

and the highest separation rate of 97% was obtained at a central maximum flux density of 6 T and flow velocity of 0.05 m/s, so the experiment was conducted under this condition. In Fig. 6, the MPs separation rate by OGMS was as low as 15%, which is lower compared to HGMS, even though 97% of the magnetite were separated for pure magnetite. Desorption of MPs and magnetite particles was considered as main reason for the low separation rate. Since the magnetic field gradient is lower in OGMS than in HGMS, the magnetic force acting on the magnetite particles should also be smaller in OGMS.

3.3. Calculation of Adhesion and Magnetic Forces Acting on The Magnetite Particle.

To compare the adhesion and magnetic forces under the respective magnetic separation conditions of OGMS and HGMS, the theoretical values of the adhesion force between MPs and magnetite particles and the magnetic force acting on the attached magnetite particles were calculated, and plotted as a function of particle size. Here, the adhesion force between MPs and magnetite particles was assumed as the combined force of Van der Waals force and electrostatic attraction due to surface charge.

Firstly, we consider the magnetic force acting on a magnetite particle. When the separation target is a ferromagnetic material such as magnetite, the magnetization of the particles reaches saturation magnetization M_s when the external magnetic field exceeds a certain value, and the magnetic force F_m is expressed in one-dimensional notation as in Equation (3),

$$F_m = \frac{4}{3} \pi r_p^3 M_s \frac{dB}{dx} \quad (3)$$

where r_p (m) is the radius of the magnetic particles and dB/dx (T/m) is the magnetic field gradient considering the magnetization of the magnetic particles.

Next, we consider the intraparticle interaction between MPs and magnetite. The potential energy of Van der Waals interaction $V_{VW(SP)}$ between heterogeneous spherical particles is expressed by Equation (4). By differentiating equation (4) by the distance between particles gives equation (5), which represents the Van der Waals force F_v acting between different particles of a spherical particle. Here, the radius of particle 1 is a_1 (m), the radius of particle 2 is a_2 (m), the distance between particles is H_0 (m), and the Hamaker constant is A (J) [11, 12]. The Hamaker constant determines the Van der Waals force between macroscopic objects, and is the order of approximately 10^{-20} (J), and varies depending on the materials.

$$V_{VW(SP)} = -\frac{Aa_1a_2}{6(a_1 + a_2)H_0} \quad (4)$$

$$F_v = \frac{dV_{VW(SP)}}{dH} = \frac{Aa_1a_2}{6(a_1 + a_2)H_0^2} \quad (5)$$

Lastly, we calculate the electrostatic attractive force acting between the particles. The interaction energy of the electric double layer of a spherical particle is expressed by Equation (6). Differentiating Equation (6) by the distance between the particles derives equation (7), which represents the interaction force of the electric double layer between spherical particles, i.e., the electrostatic attraction due to surface charges, F_E .

Here, the distance between particles is H_0 (m), the surface potential of particle 1 is ψ_{01} (V), the surface potential of particle 2 is ψ_{02} (V), and the Debye length is κ . The Debye length is a parameter that defines the degree of expanse of the ion cloud and is expressed by Equation (8). where n and ν are the number and valence of counterions in 1×10^{-6} m², respectively; e is the electronic charge; ϵ (F/m) is the dielectric constant of the solution; and k (J/K) is the Boltzmann constant [11,12].

$$V_E = \frac{\epsilon a_1 a_2 (\psi_{01}^2 + \psi_{02}^2)}{4(a_1 + a_2)} \left[\frac{2\psi_{01}\psi_{02}}{(\psi_{01}^2 + \psi_{02}^2)} \ln \frac{1 + \exp(-\kappa H_0)}{1 - \exp(-\kappa H_0)} + \ln\{1 - \exp(-2\kappa H_0)\} \right] \quad (6)$$

$$F_E = \frac{\epsilon \kappa}{2} \frac{a_1 a_2}{a_1 + a_2} \left[\frac{(\psi_{01}^2 + \psi_{02}^2) \exp(-2\kappa H_0) - 2\psi_{01}\psi_{02} \exp(-\kappa H_0)}{1 - \exp(-2\kappa H_0)} \right] \quad (7)$$

$$\kappa = \left(\frac{8\pi n e^2 \nu^2}{\epsilon k T} \right)^{1/2} \quad (8)$$

From Equation (7), it is necessary to determine the surface charge of each particle in order to consider the electrostatic attraction between MPs and magnetite particles. So the actual zeta potential measured using a microscopic electrophoresis apparatus (Model 502, Nihon Rufuto Co., Ltd., Japan) was used.

The calculated force acting on the particles is shown in Fig. 8. Based on Fig. 4, which shows the particle size distribution, the magnetite particles adhering to the MPs exist in a particle size ranged from 0.5 of primary particle size to secondary particle size (average 4.2 μ m, maximum 10 μ m), the magnetic force by OGMS does not exceed the adhesion force. However, assuming that the magnetic field is larger in OGMS than in HGMS and that magnetic aggregation occurs due to the magnetic field gradient between the particles as they are attracted to the wall surface, resulting in a secondary size of approximately 10 μ m or larger, the magnetic force acting on the particles in OGMS can be larger than the adhesion force between the MPs and magnetite. This is expected to lead to desorption of magnetite from MPs.

3.4. Separation of MPs Using Surface-Modified Magnetite.

As mentioned above, in both HGMS and OGMS, magnetite particles desorb from MPs due to magnetic force exceeding the adhesion force and the effect of magnetic aggregation, and the MPs separation rate as high as 99% obtained with batch processing magnetic separation could not be achieved in the continuous process. In this chapter, we focus on the conditions for continuous processing of MPs, i.e., adhesion force $F_A >$ magnetic force $F_M >$ drag force F_D , and investigate a magnetic separation method that does not cause desorption.

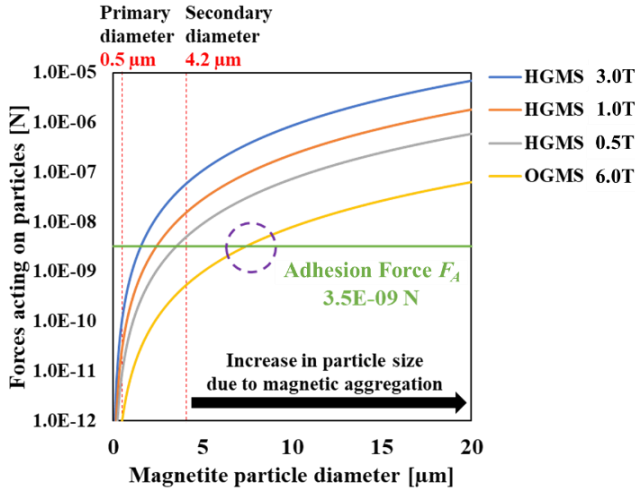


Fig. 8. Estimate of the force acting on the particle.

To increase the adhesion force between MPs and magnetite, the magnetite particles were modified with fatty acid. The surface of MPs is generally hydrophobic, hence the attractive force between MPs and magnetite increases by making the magnetite particle surface hydrophobic. In general, the hydrophobic interaction is stronger than the Van der Waals force.

Table III shows the surface modifiers of magnetite used in this study, and Table IV shows the contact angles of water on MPs and magnetite treated with each surface modifier. In this experiment, caprylic acid, one of the linear fatty acids, was used as a modifying group, because it has dispersibility in water while having some hydrophobicity. In fact, stearic and oleic acid-modified magnetite with contact angles exceeding 100° were too hydrophobic, so it stays on the water surface and did not disperse in water even when strongly stirred.

Magnetic separation experiments of HGMS were performed using fatty acid-modified magnetite particles prepared. Magnetic separation experiments using untreated magnetite particles was also conducted as a control experiment. Experimental conditions are shown in Table V. The highest MPs separation rate was obtained at 0.5 T for HGMS as shown in Fig. 6, but separation rate of pure magnetite was maximum and almost 100% at the magnetic field of 1.0 T, so the magnetic field was set to 1.0 T.

The MPs separation rate by HGMS using fatty acid-modified magnetite is shown in Fig. 9. The caprylic acid-modified magnetite achieved an 85% of MPs separation rate, with a 5% efflux rate. The significant increase in separation rate compared to untreated magnetite particles suggests that hydrophobic interactions increased adhesion force between MPs and magnetite, which prevented desorption of the particles. These results indicate that the use of hydrophobic magnetite particles as magnetic seeding agents, which are dispersible in water and have moderate hydrophobicity, can increase the interparticle interaction between MPs and magnetite and prevent desorption during continuous magnetic separation.

The surface modification of magnetite with fatty acids is a simple process, and if a technology can be established to separate magnetite from MPs after magnetic separation,

TABLE III
FATTY ACIDS USED IN THE EXPERIMENTS.

Name	Molecular weight (g/mol)	Chemical formula
Sodium Propionate	96	$\text{CH}_3\text{CH}_2\text{COO}^-$
Sodium Caprylate	166	$\text{CH}_3(\text{CH}_2)_6\text{COO}^-$
Ammonium Stearate	301	$\text{CH}_3(\text{CH}_2)_{16}\text{COO}^-$
Potassium Oleate	320	$\text{CH}_3(\text{CH}_2)_7\text{CH}=\text{CH}(\text{CH}_2)_7\text{COO}^-$

TABLE IV
CONTACT ANGLES OF MPs AND SURFACE MODIFIED MAGNETITE.

		Contact angle ($^\circ$)
MPs	PE (polyethylene)	124
	PA (polyamide)	95
Magnetite	Untreated	0
	Sodium Propionate	14
	Ammonium Stearate	132
	Potassium Oleate	128

TABLE V
EXPERIMENTAL CONDITIONS FOR HGMS USING FATTY ACID MODIFIED MAGNETITE.

MPs concentration	0.1 g/L
MPs Type	PA (Polyamide)
MPs diameter	10 μm
Magnetite concentration	0.1 g/L (100 ppm)
Magnetite primary diameter	0.5 μm (Sample B)
Flow rate	0.1 m/s
Water amount	10 L
Flow diameter	52 mm
Stirring time	20 min
Velocity	0.10 m/s
Central maximum magnetic field	1.0 T

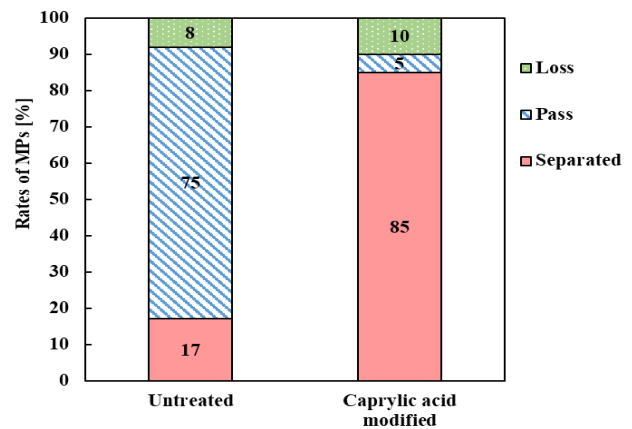


Fig. 9. Separation rate of MPs by HGMS using fatty acid modified magnetite.

there is a possibility that surface-modified magnetite particles can be reused.

4. CONCLUSION

As an advanced treatment for the removal of MPs in a sewage treatment, the conditions for the continuous separation of MPs by a magnetic separation system using the magnetic seeding method were investigated. Continuous magnetic separation experiments were conducted using a superconducting solenoidal magnet, and the appropriate conditions for continuous treatment were investigated based on the separation rate of MPs.

MPs separation rates of 55% and 15% were obtained with HGMS and OGMS, respectively, and these rates were clearly lower than the 99% separation rate obtained with small scale batch processing in our previous study. It is considered due to desorption of magnetite particles from MPs caused by a large magnetic force against the electrostatic adhesion force between MPs and magnetite. Based on the results, we prepared magnetite particles with hydrophobic surface by modification with fatty acids, and conducted the magnetic separation experiments using these particles. 85% of MPs separation rate was achieved with the fatty acid-modified magnetite particles, indicating the feasibility of continuous treatment of MPs. In the future, we plan to study the system design for mass treatment to introduce this process into sewage treatment plants. Although this experiment was conducted at concentrations of 100-500 mg/L, the effluent standard for sewage in Japan is several tens of mg/L. Thus, the amount of microplastics discharged that cannot be removed by current sewage treatment process is thought to be several tens of mg/L, which must be reduced to a few mg/L. Therefore, based on this study, the development of a magnetic separation system capable of high-efficiency treatment at low concentrations in addition to massive processing is required in the future.

REFERENCES

- [1] P. Farrell, K. Nelson, "Trophic level transfer of microplastic: *Mytilus edulis* (L.) to *Carcinus maenas* (L.)", *Environmental Pollution*, Vol.177, pp.1-3, 2013.
- [2] O. Setälä: "Ingestion and transfer of microplastics in the planktonic food web", *Environmental Pollution*, Vol.185, pp.77-83, 2014.
- [3] L. A. Holmes, A. Turner, R. C. Thompson, "Adsorption of trace metals to plastic resin pellets in the marine environment", *Environmental Pollution*, Vol.160, pp.42-48, 2012.
- [4] K. Ashton, L. Holmes, A. Turner, "Association of metals with plastic production pellets in the marine environment", *Marine Pollution Bulletin*, Vol.60, Issue.11, pp.2050-2055, 2010.
- [5] A. A. Horton, A. Walton, D. J. Spurgeon, E. Lahive, C. Svendsen: "Microplastics in freshwater and terrestrial environments: Evaluating the current understanding to identify the knowledge gaps and future research priorities", *Science of The Total Environment*, Vol.586, pp.127-141, 2017.
- [6] S. Tanaka, M. Kakita, S. Yukioka, Y. Suzuki, S. Fujii, H. Takada, "Behavior of microplastics in wastewater treatment processes and estimation of its loading to lake Biwa", *Journal of Japan Society of Civil Engineers*, Ser. G (Environmental Research), 75(7) III_35-III_40, 2019.
- [7] K. Tanaka, H. Takada, "Microplastic fragment and microbeads in digestive tracts of planktivorous fish from urban coastal waters", *Scientific reports*, Vol.6, Article number:34351, 2016.
- [8] R. Ueda, Y. Akiyama, M. Oya, "Study on Removal of Microplastics Using Magnetic Separation", *The abstract book of 11th International Forum on Magnetic Force Control (IFMFC2020)*, Oct. 23-24, 2020.
- [9] J. Yamamoto, T. Mori, Y. Akiyama, H. Okada, N. Hirota, H. Matsuura, S. Namba, T. Sekine, F. Mishima, S. Nishijima, "Removal of iron scale from boiler feed-water in thermal power plant by magnetic separation: large-scale experiment", *IEEE Transactions on Applied Superconductivity*, Vol. 29, No. 5, 2019.
- [10] T. Mori, J. Yamamoto, Y. Akiyama, H. Okada, N. Hirota, H. Matsuura, S. Namba, T. Sekine, F. Mishima, S. Nishijima, "Removal of Iron Oxide Scale from Feed-Water in Thermal Power Plant by High-Gradient Magnetic Separation: Scale-Up Effect", *IEEE Transactions on Magnetics*, Vol. 56, No. 12, 2020.
- [11] S. Shirai, "Interaction between particles and surface forces in liquids", *Journal of Materials Property Science*, Vol. 2, No. 1, pp.171-180, 1989.
- [12] J. N. Israelachvili, "Intermolecular and Surface Forces", 2nd Edition, Asakura Publishing Co., Ltd., Tokyo, pp172-276, 1996.